# Asymmetric velocity correlations in shearing media

Peter Olsson
*Department of Physics, Umeå University, 901 87 Umeå, Sweden*
(Received 12 May 2010; published 3 September 2010)

A model of soft frictionless disks in two dimensions at zero temperature is simulated with a shearing dynamics to study various kinds of asymmetries in sheared systems. We examine both single particle properties, the spatial velocity correlation function, and a correlation function designed to separate clockwise and counterclockwise rotational fields from one another. Among the rich and interesting behaviors we find that the velocity correlation along the two different diagonals corresponding to compression and dilation, respectively, are almost identical and, furthermore, that a feature in one of the correlation functions is directly related to irreversible plastic events.

DOI: 10.1103/PhysRevE.82.031303 PACS number(s): 45.70.−n, 64.60.−i

## I. INTRODUCTION

In collections of particles with repulsive contact interaction there is a transition from a liquid to an amorphous solid state as the volume fraction increases—the jamming transition. It has been suggested that this transition is a critical phenomenon with universal critical exponents [1] and the successful scaling of rheology data from simulations is strong evidence that that actually is the case [2–4]. The precise values of the critical exponents, however, continue to be a matter of discussion [5].

At the very heart of critical phenomena is the notion of a correlation length that diverges as the critical point is approached. It is therefore important to identify the proper correlation length. Several works have tried to look for a growing order in the static quantities, but without much success. Another possibility is to look for a growing length in the dynamics. Velocity correlations in sheared systems were studied in Ref. [6] though not revealing any growing length. A large correlation length was however found in Ref. [7] and they also argued for a pronounced angular dependence of the velocity correlations [8].

In a previous work we reported the finding of a growing characteristic length from the transverse component of the velocity correlation function [2]. The extraction of the correlation length exponent, however, seems to be more complicated than presented there and we therefore set out to do a more thorough analysis of the velocity correlations. As an important step in that direction we here consider some symmetry properties of velocity correlations in a sheared system and find a surprisingly rich and interesting behavior.

When shearing simulations are done slowly enough it becomes possible to separate the time evolution into elastic parts where the energy slowly increases and plastic contributions which are irreversible processes where the system rapidly evolves and dissipates energy [9]. We will argue below that the contribution from the plastic processes also may be seen in a certain velocity correlation function.

The content of the present paper is the following: in Sec. II we briefly describe the model and the simulations. Section III describes some rather direct measures of velocity correlations and how they depend on the direction of the separation between the particles whereas Sec. IV deals with a more involved correlation function designed to capture the difference between clockwise and counterclockwise rotations of the velocity field. A summary and some concluding remarks are given in Sec. V.

## II. MODEL AND SIMULATIONS

Following O'Hern *et al.* [10] we simulate frictionless soft disks in two dimensions using a bidispersive mixture with equal numbers of disks with two different radii of ratio 1.4. Length is measured in units of the small particles ($d_s=1$). With $r_{ij}$ for the distance between the centers of two particles and $d_{ij}$ the sum of their radii, the interaction between overlapping particles is

$$V(r_{ij}) = \begin{cases} \frac{\epsilon}{2}(1 - r_{ij}/d_{ij})^2, & r_{ij} < d_{ij}, \\ 0, & r_{ij} \geq d_{ij}. \end{cases} \quad (1)$$

We use Lees-Edwards boundary conditions [11] to introduce a time-dependent shear strain $\gamma = t\dot{\gamma}$. With periodic boundary conditions on the coordinates $x_i$ and $y_i$ in an $L \times L$ system, the position of particle $i$ in a box with strain $\gamma$ is defined as $\mathbf{r}_i = (x_i + \gamma y_i, y_i)$ which thus gives a shear flow in the $x$ direction. We simulate overdamped dynamics at zero temperature with the equation of motion [12],

$$\frac{d\mathbf{r}_i}{dt} = -C\sum_j \frac{dV(\mathbf{r}_{ij})}{d\mathbf{r}_i} + y_i\dot{\gamma}\hat{x},$$

which is integrated with the second order Heuns' method.

This above expression is for the total velocity, including the shearing part. In the analyzes of the velocity correlations below we will use the nonaffine part of the velocity excluding the trivial shearing part $y_i\dot{\gamma}\hat{x}$. This nonaffine part of the velocity will be denoted by $\mathbf{v}$. Our simulations are performed with $N=65536$ particles and shear rates down to $\dot{\gamma} = 10^{-8}/\tau_0$ where $\tau_0 = d_s/C\epsilon$ is the unit of time.

Our dynamic model here is just the Durian bubble model [12] where the dissipation is caused by the velocity difference of particles in contact. Following Durian, we use a mean-field-like (MF) approximation: for the equation of motion of particle $i$ we replace the particular velocities of the

 

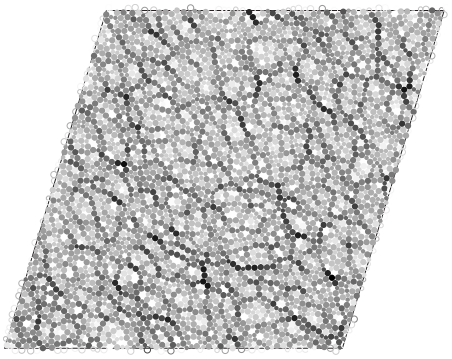

FIG. 1. Configuration with 4096 particles color coded according to the elastic energy of each particle. The dark particles (high elastic energy) make up force chains that preferably extend along the $\hat{x}-\hat{y}$ direction.

particles in contact with particle $i$ with the steady state average velocity of the system at the position of particle $i$. This has commonly been believed to be a good approximation, especially at low shearing rates. This MF model is, in a sense, the simplest of all dynamical models, and is therefore in our opinion worthy of study in its own right. We note, however, that recent work has claimed that the velocity correlations, that are the subject of this paper, may be quite sensitive to this MF approximation [5]. We question that conclusion but leave this to further investigation and proceed here with the analysis of our MF dynamics.

## III. VELOCITY CORRELATIONS

### A. Symmetry of a shearing system

Figure 1 shows the presence of force chains in our shearing system. The figure is a configuration with 4096 particles, color coded according to the elastic energy of each particle. As is well known, the force chains [8] tend to be along the $\hat{x}-\hat{y}$ direction, which is the direction of compression. This means that the force chains break the reflection symmetry along $x$ and that the system is only symmetric under the *combined* transformation $x\to -x$ and $y\to -y$. The same conclusion is readily drawn from the expression for the shear stress,

$$\sigma = \frac{1}{L^2}\sum_{ij} f_{ij}^x y_{ij},$$

where $L$ is the linear system size, the sum is over pairs of particles, $f_{ij}^x$ is the $x$ component of the force between particles $i$ and $j$, and $y_{ij}$ is the $y$ component of their separation. Note that the shear stress changes sign under the transformation $x\to -x$ but remains unchanged under the combined transformation $x\to -x$ and $y\to -y$.

### B. Single particle properties

As we will see below several symmetries that hold in systems at equilibrium are broken in a shearing system. The simplest symmetry is however respected; there is no net velocity in the system, $\langle \mathbf{v}\rangle = 0$. As remarked above, $\mathbf{v}$ is the

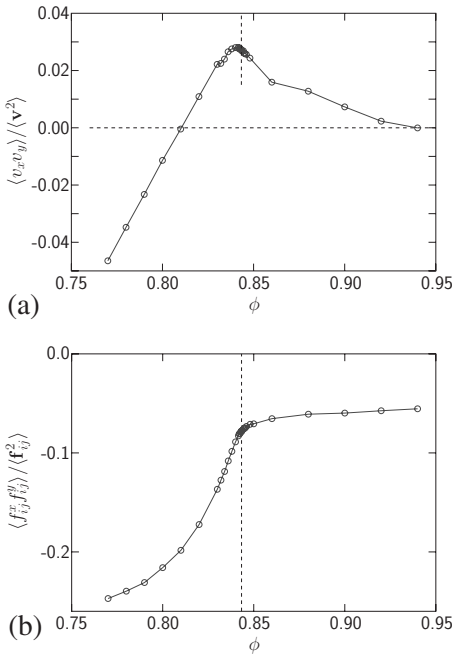


FIG. 2. Measure of the anisotropy in both particle velocities and contact forces from simulations with $\dot{\gamma}=10^{-7}$. Panel (a) shows the normalized $\langle v_x v_y\rangle$ for individual particles versus density. The correlation changes from negative at low densities to positive around $\phi \approx \phi_J$ (dashed vertical line), signifying a change from a predominance of motion along the force chains to a slight overweight for motion perpendicular to the force chains. Panel (b) shows that the corresponding contact force correlation is always negative, which is consistence with the existence of force chains at all densities. This contact force correlation also has a marked feature at $\phi \approx \phi_J$.

nonaffine part of the velocity. Here and in the following $\langle \ldots \rangle$ represents the average over all particles and a large number of configurations generated with our shearing dynamics. For the average velocity things are unusually simple since this result holds for each individual configuration as a consequence of the overdamped dynamics and total force balance, $\mathbf{v}=\Sigma_i \mathbf{v}_i = C\Sigma_{ij}\mathbf{f}_{ij}=0$ as $\mathbf{f}_{ij}=-\mathbf{f}_{ji}$.

The conclusion of a vanishing average velocity may also be reached from the symmetry considerations. Since the combined transformation also implies the change of sign of both velocity components, $v_x\to -v_x$ and $v_y\to -v_y$, it follows that $\langle v_\mu\rangle = \langle -v_\mu\rangle$, for $\mu = x,y$, which gives $\langle v_\mu\rangle = 0$.

In contrast to equilibrium results from symmetry that $\langle v_x v_y\rangle = 0$, one finds that this quantity does not vanish in the sheared system. Figure 2 shows $\langle v_x v_y\rangle / \langle \mathbf{v}^2\rangle$ against $\phi$. At low densities the correlation is negative which means that the particles tend to move more along than perpendicular to the force chains. The correlation changes sign at $\phi \approx 0.81$, reaches a peak at $\phi \approx 0.84 \approx \phi_J$ and then decrease toward zero. This means that there is a region around $\phi_J$ where the particles move slightly more in the direction *perpendicular to* the force chains.

A related quantity is $\langle f_{ij}^x f_{ij}^y\rangle$ which is the correlation between the different components of the contact force $\mathbf{f}_{ij}$. Note that there is a direct relation between the velocities and the contact forces: $\mathbf{v}_i = C\Sigma_j \mathbf{f}_{ij}$, where the sum extends over all particles $j$ in contact with $i$. Nevertheless, $\langle f_{ij}^x f_{ij}^y\rangle$ behaves

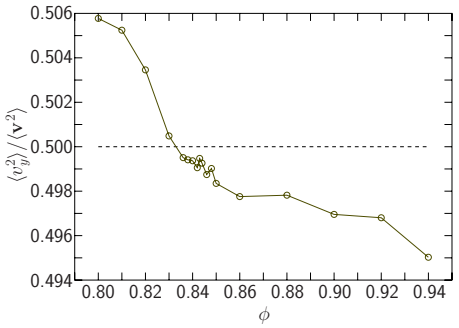


FIG. 3. (Color online) The anisotropy measured through the $\langle v_y^2\rangle$ relative to $\langle \mathbf{v}^2\rangle = \langle v_x^2\rangle + \langle v_y^2\rangle$. This fraction is close to 50% in the regions around jamming but decreases slightly with increasing density.

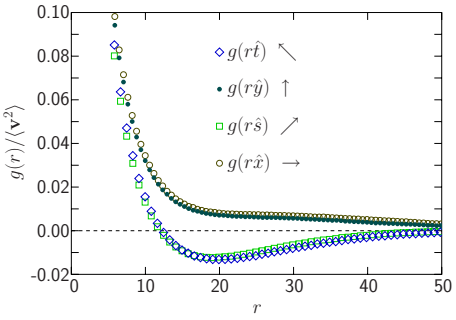


FIG. 4. (Color online) Total velocity correlation along the four different main directions. The decay of the correlations is monotonic along the main directions, $\hat{x}$ and $\hat{y}$ and nonmonotonic along the diagonals. This is for $\phi = 0.8433 \approx \phi_J$ and shear rate $\dot{\gamma} = 10^{-6}$.

rather differently from the velocity correlations. Whereas $\langle v_x v_y\rangle/\langle \mathbf{v}^2\rangle$ has a peak at $\phi \approx \phi_J$, Fig. 2(b) shows that the normalized $\langle f_{ij}^x f_{ij}^y\rangle$ changes at the same density from a rapid increase (which is a *decrease* in magnitude) to being almost constant.

Another measure of the asymmetry is the relative magnitude of the two velocity components. From energy balance—that the dissipated power has to be equal to the supplied power—follows the result for the velocity squared: $C\langle \mathbf{v}^2\rangle = (L^2/N)\sigma\dot{\gamma}$ [6]. This dissipated power needs however not be equal in the $x$ and $y$ directions. Figure 3 shows that the fraction of the power dissipated by velocities along the $y$ direction is close to 50%, but also that there is a clear dependence on density: $\langle v_y^2\rangle/\langle \mathbf{v}^2\rangle$ decreases from 0.506 to 0.495 when the density increases from $\phi = 0.80$ to 0.94.

### C. Spatial dependence

We now turn to the spatial velocity correlations, i.e., the correlations between pairs of particles with separation $\mathbf{r}$. We first focus on the total correlation function,

$$g(\mathbf{r}) = \langle \mathbf{v}(\mathbf{r}') \cdot \mathbf{v}(\mathbf{r}' + \mathbf{r})\rangle, \tag{2}$$

and examine how it depends on both magnitude $r = |\mathbf{r}|$ and direction of $\mathbf{r}$. We will study this correlation function in four different directions: along the two main directions, $\hat{x}$, $\hat{y}$, and along the diagonals

$$\hat{s} = (\hat{x} + \hat{y})/\sqrt{2},$$

$$\hat{t} = (\hat{y} - \hat{x})/\sqrt{2}.$$

In our shearing geometry $\hat{t}$ is the direction of uniaxial compression and $\hat{s}$ the direction of uniaxial dilation. Figure 4 shows the correlation functions obtained with $\phi = 0.8433 \approx \phi_J$ and $\dot{\gamma} = 10^{-6}$ along these four different directions. The curves are pairwise equal with, on the one hand, the correlations along the main directions, $\hat{x}$ and $\hat{y}$, and on the other hand the correlations along the diagonals. These results should be essentially without finite size effects since the system size is $L \approx 300$ whereas $r$ only extends up to 50. In view of the density dependence in Figs. 2 and 3 we have confirmed that the general behavior remains the same for a wide range of densities around $\phi_J$.

The result that $g(\mathbf{r})$ behaves the same along both diagonals is different from the earlier finding of an angular dependence of the correlation length in shearing systems [7] with minimum and maximum along the different diagonals. The reason for this difference is not clear, but we speculate that it is related to the very different dynamics in their system, which is also reflected in the oscillatory behavior of their velocity correlation function.

To investigate the reason for the dependence of $g(\mathbf{r})$ on the direction of $\mathbf{r}$, we separate the correlations into longitudinal and transverse components, parallel and perpendicular to the separation, respectively. In the $x$ direction these components are

$$g_{\parallel}(r\hat{x}) = \langle v_x(0) v_x(r\hat{x})\rangle,$$

$$g_{\perp}(r\hat{x}) = \langle v_y(0) v_y(r\hat{x})\rangle,$$

with obvious generalizations to the other directions. After this separation we find that the transverse component along these four different directions behaves about the same, see Fig. 5(a). (The rather small differences in the transverse component for the two diagonal directions will be discussed further below.) The difference is largely due to the decay of the longitudinal component, Fig. 5(b), which is monotonic along the main ($\hat{x}$ and $\hat{y}$) directions but nonmonotonic along the diagonals.

The result above is a different behavior along the diagonals compared to the main directions. We now instead focus on the difference between the two diagonal directions, $\hat{s}$ and $\hat{t}$. From Fig. 4 we found that the total velocity correlations along these two directions are very similar. Nevertheless, as shown in Fig. 5 both $g_{\parallel}$ and $g_{\perp}$ are clearly different. This suggests that this difference originates from the mixed correlations $g_{xy}(\mathbf{r}) = \langle v_x(0) v_y(\mathbf{r})\rangle$. To see this we use the definitions $g_{\parallel}(r\hat{s}) = \langle v_s(0) v_s(r\hat{s})\rangle$, and $g_{\perp}(r\hat{s}) = \langle v_t(0) v_t(r\hat{s})\rangle$ together with $v_s = (v_x + v_y)/\sqrt{2}$ and $v_t = (v_y - v_x)/\sqrt{2}$ for the velocities along the diagonals. This gives

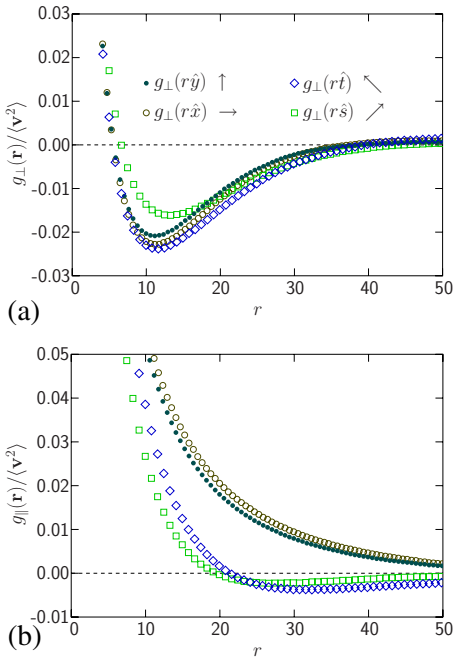


FIG. 5. (Color online) Transverse and longitudinal velocity correlations, respectively, along the four different directions. The transverse correlation in panel (a) is very similar for all four directions whereas the longitudinal correlation function shown in panel (b) is different for the diagonal directions, compared to the two main directions. The differences in the total velocity correlations in Fig. 4 are thus related to differences in the longitudinal correlations.

$$g_{\parallel}(r\hat{s}) = g(r\hat{s}) + g_{yx}(r\hat{s}),$$

$$g_{\perp}(r\hat{s}) = g(r\hat{s}) - g_{yx}(r\hat{s}),$$

where we have also made use of the symmetry $g_{xy}=g_{yx}$ which follows from considering the transformation $\mathbf{r}\to-\mathbf{r}$, followed by a translation: $v_x(0)v_y(\mathbf{r})\to[-v_x(0)][-v_y(-\mathbf{r})]=v_x(\mathbf{r})v_y(0)=v_y(0)v_x(\mathbf{r})$.

Figure 6 shows the mixed correlations along the two diagonal directions. The thick arrows in the inset illustrate the velocity fields one might expect as an effect of a particle with $v_y>0$ which is $v_x>0$ for separations in the $\hat{s}$ direction and $v_x<0$ in the $\hat{t}$ direction. Since we expect $v_x<0$ along $\hat{t}$, the correlations in that direction are shown with the opposite sign. Note that both functions start out at $g_{yx}(0)=\langle v_x v_y\rangle$. The correlations then grow above this $r=0$ value and actually become stronger in the $\hat{t}$ direction (though with opposite sign) than along $\hat{s}$. For a comparison, the dashed lines are the correlations of $v_y$ along the same directions. This difference between $g_{yx}(r\hat{s})$ and $-g_{yx}(r\hat{t})$ is yet another example of a broken symmetry in the shearing system.

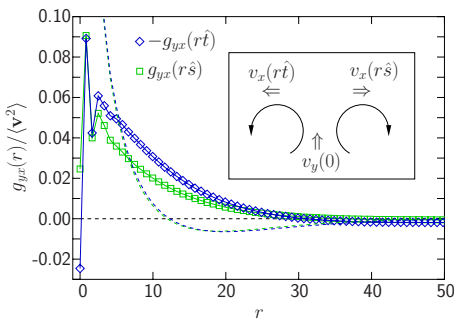


FIG. 6. (Color online) The mixed correlation functions $g_{yx}(r\hat{s})$ and $-g_{yx}(r\hat{t})$. The difference between the mixed correlation functions (apart from the trivially different sign) is yet an example of the asymmetry in the sheared system. The arrows in the inset illustrate the rotational velocity fields which have the effect that a velocity $v_y(0)>0$ at the origin on the average gives $v_x(r\hat{s})>0$ and $v_x(r\hat{t})<0$.

## IV. ROTATIONAL ASYMMETRY

The previous section gave evidence for the importance of whirls in the velocity field. The inset of Fig. 6 shows two such whirls that are a consequence of $v_y(0)>0$, and there will also be whirls with the opposite orientation that will contribute to the correlation functions in much the same way. The question we now like to address is whether they contribute equally much or not. Is the system symmetric when considering whirls with clockwise and counterclockwise rotations, respectively?

Since the shearing by itself introduces a rotational field, it could at first seem obvious that this symmetry is broken, but that is not correct. Our velocity correlations are calculated from the *nonaffine* velocities and the net rotation is zero in the nonaffine velocity field. The system could therefore in principle well be symmetric with respect to these different directions of rotation.

### A. Asymmetric correlations

There are at least two different ways to motivate the new correlation function that we are about to introduce. The first is to note that the direction of the rotational fields in the inset of Fig. 6 depend on the sign of $v_y(0)$. With the opposite sign of $v_y(0)$, $v_x(r\hat{t})$, and $v_x(r\hat{s})$ would also (typically) change sign and the rotations would be in the opposite directions.

A second point of departure is to consider the fact that the correlation function defined in Eq. (2) is symmetric under the transformation $x\to-x$ whereas the system itself is only symmetric under the interchange of both $x$ and $y$. This suggests that some information is lost when calculating the standard correlation function and, furthermore, that a guiding principle in the definition of an ideal correlation function is that it should have the same symmetry as the system.

It is then possible to combine both these lines of thought and construct a function by restricting the average in Eq. (2) to only include terms with $v_y(\mathbf{r}')>0$. For the transverse correlation function with $\mathbf{r}$ along the $\hat{x}$ direction, this becomes

$$g_{\perp}^{+}(x) = \langle v_y(\mathbf{r}')v_y(\mathbf{r}'+x\hat{x})\rangle_{v_y(\mathbf{r}')>0}. \quad (3)$$

This expression may further be generalized to including particles with both signs of $v_y(\mathbf{r})$ by letting the direction of the separation ($+x\hat{x}$ or $-x\hat{x}$) depend on the sign of the velocity,

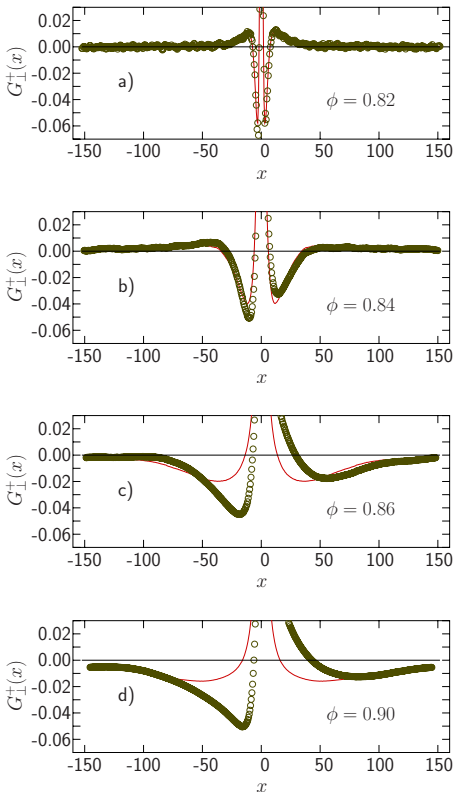


FIG. 7. (Color online) Development of the asymmetry in $G_\perp^+(x)$. The function is nearly symmetric at $\phi=0.82$ but develops a very pronounced asymmetry as the density is increased above $\phi_J$. The solid lines are the symmetric $G_\perp$. The shear rate is $\dot{\gamma}=10^{-7}$.

$$g_\perp^+(x) = \frac{1}{N_{\text{term}}} \sum_{\mathbf{r}'} \begin{cases} v_y(\mathbf{r}')v_y(\mathbf{r}'+x\hat{x}), & v_y(\mathbf{r}') > 0, \\ v_y(\mathbf{r}')v_y(\mathbf{r}'-x\hat{x}), & v_y(\mathbf{r}') < 0. \end{cases} \quad (4)$$

The normalization $N_{\text{term}}$ is the number of terms in the sum. Written this way it becomes clear that $g_\perp^+(x)$ indeed has the desired symmetry properties. The rational for this new asymmetric function is also discussed in conjunction with Fig. 11. Note also that the *symmetric* function is related to $g_\perp(x)$ through

$$g_\perp(x) = \frac{1}{2}[g_\perp^+(x) + g_\perp^+(-x)].$$

The quantities shown in the figures below (both symmetric and asymmetric) are, $G(x)=g(x)/g(0)$, normalized such that $G(0)=1$.

Figure 7 shows $G_\perp^+(x)$ at four different densities both above and below $\phi_J$, again from simulations with $\dot{\gamma}=10^{-7}$. For comparison, the symmetrized function $G_\perp(x)$ is given by the solid line. At $\phi=0.82$, panel (a), $G_\perp^+(x)$ is almost symmetric. The other panels show that the asymmetry grows with increasing $\phi$, and at $\phi=0.90$ well above $\phi_J$, panel (d), the asymmetry is very pronounced. The $x<0$ part shows a sharp dip at $x\approx-18$ whereas the $x>0$ part has a rather shallow minimum at $x\approx 79$.

Another way to illustrate the growth of the asymmetry is through the position of the minima. Figure 8 shows $\ell_+$ and

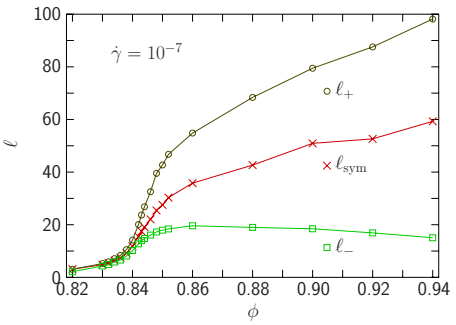


FIG. 8. (Color online) Location of the respective minima of the correlation functions. $\ell_+$ and $\ell_-$ are the positions of the minima of $G_\perp^+$ at $x>0$ and $x<0$, respectively, whereas $\ell_{\text{sym}}$ is from the minimum of $G_\perp$. The asymmetry of $G_\perp^+$ which is reflected in the difference $\ell_+-\ell_-$ develops around $\phi_J$.

$\ell_-$, the absolute value of the position of the minima for $x>0$ and $x<0$, respectively, together with $\ell_{\text{sym}}$ from the minimum of the symmetrized function. The asymmetry grows rapidly above $\phi=0.84$ and the behavior of $\ell_+$ and $\ell_-$ turn out to be very different at higher densities; $\ell_+$ continues to increase whereas $\ell_-$ reaches a maximum at $\phi\approx 0.86$ and then decreases slowly.

Figure 9 is the same quantity obtained at $\phi=0.8433\approx\phi_J$ [13] with different shear rates. It is here found that the asymmetry grows with decreasing shear rate. The algebraic increase of $\ell_+$, which suggest a divergence in the limit of vanishing shear rate, is clear from Fig. 10 whereas both $\ell_-$ and $\ell_{\text{sym}}$ grow less rapidly.

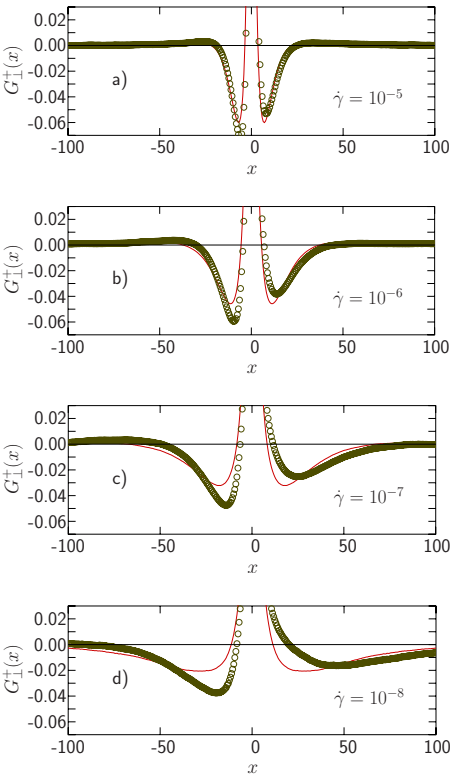


FIG. 9. (Color online) The correlation function $G_\perp^+(x)$ at $\phi=0.8433\approx\phi_J$ and several different shear rates down to $\dot{\gamma}=10^{-8}$. The asymmetry increases slowly with decreasing shear rate.

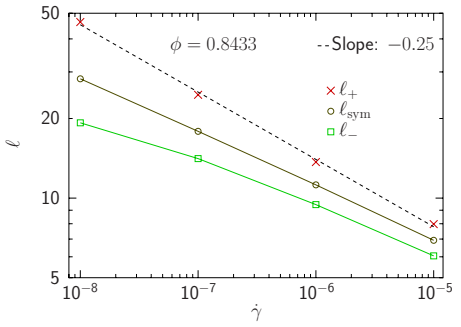


FIG. 10. (Color online) Position of the minima of $g_\perp^+(x)$ and $g_\perp$, respectively, at $\phi=0.8433\approx\phi_J$ and four different shear rates. Note the algebraic increase of $\ell_+\sim\dot\gamma^{-0.25}$ which would imply a divergence at vanishing $\dot\gamma$.

### B. Origin of the rotational asymmetry

We now turn to the question of the origin of the asymmetry in $g_\perp^+(x)$ and will argue that it is linked to the plastic processes. The reason for this is the manifest asymmetry of the velocity profile of an elementary plastic event, as shown in the inset of Fig. 11 [9]. Note that the orientation of this velocity profile with its quadrupolar structure is dictated by the direction of the shear. The velocity field corresponds to a compression along the $\pm(x-y)$ direction together with an expansion in the orthogonal $\pm(x+y)$ directions, which is equivalent to a simple shear. This implies that the mirror version of such an event is expected to be much less common, if at all present, and it is this effect that causes the asymmetry. Note that this agrees well with the enhanced anticorrelation at $x<0$. When a particle has $v_y>0$ due to a plastic event one would expect that there should be one or more other particles with $v_y<0$, and the inset of Fig. 11 shows that they should be found in the $-x$ direction.

To further check this idea we have tried to separate the contribution to the correlation function from the plastic events from the rest, i.e., we have calculated $g_\perp^+$ separately

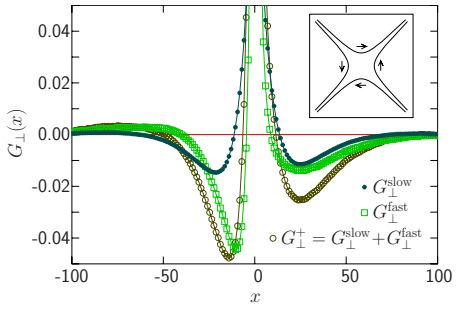


FIG. 11. (Color online) Splitting of the correlation function into two different contributions at $\phi=0.8433$ and $\dot\gamma=10^{-7}$. The total $G_\perp^+(x)$ (open circles) is split into contributions from slow and fast particles, respectively. It is clear that the asymmetry is largely an effect of the fast particles which we relate to the plastic processes. The inset shows an idealized velocity profile for a typical plastic event with quadrupolar structure. Note that this velocity field is a consequence of our shearing geometry which is equivalent to a compression along the $\pm(x-y)$ directions together with an dilation in the orthogonal $\pm(x+y)$ directions.

for increasing and decreasing total energy [6], respectively. That study, which was done for $N=4096$ particles, did indeed give evidence (not shown) that the part related to a *decrease* in total energy was the more asymmetric one. However, since the total energy is a global quantity that kind of analysis is not a very sensitive one, at least not at finite shear rates. In a large system one would expect some regions to be characterized by plastic events and a local decrease in energy whereas the motion in other regions is elastic, but we still have to classify the whole system as either plastic or elastic.

Instead of splitting up the contributions based on the change in the total energy we now consider the change in the *local* energy. That is done by classifying each term in Eq. (4) as "fast" or "slow," corresponding to plastic and elastic, respectively. Since the change in total energy is $\Delta E=L^2\sigma\dot\gamma-C\Sigma_i\mathbf{v}_i^2$ [6], the change in the local energy is related to the average $\mathbf{v}^2$ in a certain region. On the average, one expects the energy to decrease locally if $\mathbf{v}^2>\langle\mathbf{v}^2\rangle$. As a reasonable and more sensitive way to split $g_\perp^+(x)$ into two different contributions, $g_\perp^+=g_\perp^{\rm slow}+g_\perp^{\rm fast}$ (we drop the "+" in the "slow" and "fast" terms to simplify the notation) we therefore classify each of the terms in Eq. (4) according to the magnitude of the velocities. If both $\mathbf{v}(\mathbf{r}')$ and $\mathbf{v}(\mathbf{r}'+x\hat{x})$ are slow, (i.e., they both obey $\mathbf{v}^2<\langle\mathbf{v}^2\rangle$), the term contributes to $g_\perp^{\rm slow}$ whereas it contributes to $g_\perp^{\rm fast}$ otherwise, i.e., if at least one of the particles is fast.

Figure 11 shows the splitting of the total $G_\perp^+(x)$ (open circles) into slow and fast parts, respectively. Note that the contribution from the slow particles (solid dots) is almost symmetric whereas there is a very pronounced asymmetry from the fast particles (open squares). This is therefore evidence that the asymmetry is caused by the fast particles and that this typically is related to a local drop in energy which is often related to a plastic event.

## V. SUMMARY

To summarize, we have examined velocity correlations in a sheared system with emphasis on the breaking of symmetries due to the shearing. We first find that $\langle v_x v_y\rangle\neq 0$ for individual particles and that this correlation depends strongly on density. At low densities the particle preferably move *along* the force chains whereas they preferably move *perpendicular to* the force chains around $\phi_J$. We then examine how the total velocity correlation $g(\mathbf{r})$ depends on the direction of $\mathbf{r}$. Rather surprisingly, the correlation along the two diagonals, corresponding to the direction of compression and dilation, respectively, are almost identical. The decay along the diagonals is nonmonotonic, in contrast to the monotonic decay along the main ($\hat{x}$ and $\hat{y}$) directions.

We then argue that the usual correlation functions are more symmetric than the system itself and define a less symmetric velocity correlation function that also may be used to probe the differences between clockwise and counterclockwise rotations. This function is asymmetric with respect to $x$, and this is an asymmetry that increases rather dramatically when either the density increases above $\phi_J$ or the shear rate decreases at fixed $\phi\approx\phi_J$. We attribute the asymmetry to elementary plastic events with quadrupolar symmetry and their

orientation dictated by the direction of the shear as shown in the inset of Fig. 11.

This investigation of various velocity correlations has been done with the ultimate goal to determine the correlation length and the correlation length exponent. The wildly different behavior of the various correlation functions suggests that this is a nontrivial task, but things nevertheless do seem promising. As will be discussed elsewhere, we have found that a certain mixed correlation function—similar to $g_{xy}(r)$ in Fig. 6—decays exponentially over surprisingly large ranges in $r$. Another promising finding is that the same length (apart from a constant factor) shows up in the ultimate decay to zero of $g_{\|}(r\hat{x})$.

## ACKNOWLEDGMENTS

I thank S. Teitel for helpful discussions and critical reading of an earlier version of the manuscript. This work was supported by the Swedish Research Council; the computations have been performed at HPC2N under a grant provided by the Swedish National Infrastructure for Computing (SNIC).

[1] A. J. Liu and S. R. Nagel, Nature (London) **396**, 21 (1998).
[2] P. Olsson and S. Teitel, Phys. Rev. Lett. **99**, 178001 (2007).
[3] T. Hatano, J. Phys. Soc. Jpn. **77**, 123002 (2008).
[4] M. Otsuki and H. Hayakawa, Phys. Rev. E **80**, 011308 (2009).
[5] B. P. Tighe, E. Woldhuis, J. J. Remmers, W. van Saarloos, and M. van Hecke, Phys. Rev. Lett. **105**, 088303 (2010).
[6] I. K. Ono, S. Tewari, S. A. Langer, and A. J. Liu, Phys. Rev. E **67**, 061503 (2003).
[7] G. Lois, A. Lemaître, and J. M. Carlson, Phys. Rev. E **76**, 021302 (2007).
[8] T. S. Majmudar and R. P. Behringer, Nature (London) **435**, 1079 (2005).
[9] C. Maloney and A. Lemaître, Phys. Rev. Lett. **93**, 016001 (2004).
[10] C. S. O'Hern, L. E. Silbert, A. J. Liu, and S. R. Nagel, Phys. Rev. E **68**, 011306 (2003).
[11] D. J. Evans and G. P. Morriss, *Statistical Mechanics of Nonequilibrium Liquids* (Academic Press, London, 1990).
[12] D. J. Durian, Phys. Rev. Lett. **75**, 4780 (1995).
[13] C. Heussinger and J.-L. Barrat, Phys. Rev. Lett. **102**, 218303 (2009).